$D1R^{CaMKII}$ in claustrum mediates adolescent cocaine exposure-induced anxiety and electro-acupuncture therapy

Liying Chen[1,2,5], Yu Fan[1,5], Zhaoyu Liu[1], Ziheng Zhao[1], Demin Du[1], Weichao Pan[1], Xiaoyan Wei[1], Jiaxun Nie[1], Feifei Ge[1], Jianhua Ding[3], Hee Young Kim[4,*], Xiaowei Guan[1,*]

[1]Department of Human Anatomy and Histoembryology, Nanjing University of Chinese Medicine, Nanjing, China

[2]Department of Critical Care Medicine, Jiangxi Province Hospital of Integrated Chinese and Western Medicine, Nanchang, China

[3]Department of Pharmacology, Nanjing Medical University, Nanjing, China

[4]Department of Physiology, Yonsei University College of Medicine, Seoul, South Korea

[5]These authors are equally contribute to this work

Running title: Claustrum $D1R^{CaMKII}$ in ACE anxiety and EA

* Correspondence authors: guanxw918@njucm.edu.cn (XG), vet202001@yuhs.ac (HYK)

Phone number: +86-25-85811387

Highlights

- Adolescent cocaine exposure (ACE) evokes claustrum and $D1R^{CaMKII}$ in mice of adulthood.
- $D1R^{CaMKII}$ is required for ACE-induced anxiety through mediating claustrum activity.
- By targeting claustral $D1R^{CaMKII}$, EA rescues ACE-induce claustrum activation and anxiety.

Abstract

Adolescent cocaine exposure (ACE) increases risk of developing psychiatric problems such as anxiety later in life. Here, ACE animal models were established by exposing to cocaine during adolescent period in male mice, followed by electro-acupuncture (EA) at acupoints of GV 20 and GV 29 with stimuli of a mixed frequency of 2/100 Hz for 28 withdrawal days. Elevated plus maze (EPM) etc. behavioral tests were used to assess anxiety in mice. SCH23390 and specific knocking-down virus were used to regulate dopamine receptor 1 (D1R) on CaMKII-positive neurons ($D1R^{CaMKII}$) of claustrum *in vivo*. ACE mice of adulthood exhibited anxiety-like behaviors, accompanying with obviously activated CaMKII-positive neurons and increased $D1R^{CaMKII}$ in claustrum. Blocking D1R or knocking-down of $D1R^{CaMKII}$ within claustrum efficiently reduced claustrum activation, and ultimately suppressed anxiety in ACE mice of adulthood. EA treatment alleviated ACE-induced anxiety by suppressing $D1R^{CaMKII}$ and claustrum activation. Our findings identified a novel role of claustrum in ACE-induced anxiety, and put new insight into the function of claustral $D1R^{CaMKII}$. Targeting claustral $D1R^{CaMKII}$, EA obviously alleviates ACE-induced anxiety in mice of adulthood.

Keywords: Adolescent cocaine exposure; Anxiety; Claustrum; $D1R^{CaMKII}$; Electro-acupuncture

1. Introduction

Adolescents present higher vulnerability to substance abuse [1,2]. Adolescent experience of drugs increase the risk of developing psychiatric disorders that even persists into adulthood [3,4]. Anxiety is a prominent psychiatric symptom of adolescent drug abuse, which is generally believed as critical factor for driving relapse to drugs in later life [5,6]. Previously, we showed that adolescent cocaine-exposed (ACE) mice exhibit more anxiety in their adulthood [7,8], however, the involved brain region remains much to be clarified.

The claustrum is a thin stripped nucleus located between insular cortex and putamen, being architected in anterior-posterior and dorsal-ventral organization. Above 90% neurons in claustrum are glutamatergic (CaMKII-positive) neurons [9,10]. Anatomically, the claustrum has extensive reciprocal connectivity with all neocortical regions [11] and communicates densely with limbic structure and thalamus [12,13], implying that claustrum may be a hub for integrating and relaying “executive process” of cortex. At present, the functions of claustrum remain poorly understood. Emerging studies demonstrate that claustrum may be key nucleus involved in consciousness [14], attention [15] and cognition [16]. The claustrum has been implicated in numerous brain disorders, such as seizures [17], autism [18] and Parkinson Disease [19], but it has not been evidently as the core structure of any specific disease. In marijuana addicts [20,21] or internet game addicts [22], the claustrum shows greater activity. Recently, Terem et al. [23] found that the D1 dopamine receptor (D1R)-positive neurons in claustrum is required for acquisition of cocaine-preferred behaviors, and stimulating these neurons could drive context-reinstatement of cocaine preference. In addition, the other recent study shows that the claustrum

mediates stress-induced anxiety in mice [24]. These studies demonstrate that claustrum is involved in both addiction and anxiety, but its role in drugs-related anxiety is unknown.

Currently, there is few pharmacotherapy options for adolescent substance use-induced anxiety, partially due to serious side-effects caused by anxiolytic medicine. As a non-invasive therapeutic approach, acupuncture has been considered as an efficient intervention on substance use, especially for treatment of the protract abstinence syndrome (such as anxiety) [25,26], but its pharmacological targets remain largely unclear. The electro-acupuncture (EA), a kind of peripheral acupuncture with electric stimulation, has been shown to improve anxiety without adverse effects [27,28]. Previously, we found that EA at acupoints of Baihui (GV 20) and Yintang (GV 29) effectively reduced the anxiety in ACE mice of adulthood [29]. Early in 2006, Shapo et al. [30] reported that acupuncture at Weizhong points (BL40) could significantly evoke claustrum in humans. Whether claustrum is one of key targets for EA to treat ACE-related anxiety, and its potential pharmacological mechanism, has not been explored yet.

In the present study, male mice were exposed to cocaine during adolescent period from postnatal day 28 (P28) to P42 [31], followed by subsequent EA treatment. When growing up to adult age, the mice were subjected to anxiety behavioral tests to explore the role of claustral D1R, especially expressed on CaMKII-positive neurons ($D1R^{CaMKII}$), in ACE-induced anxiety and EA therapy.

2. Materials and methods

2.1 Animals

Male C57BL/6 wild type (WT) mice weighing 12-16 g were used. All animals were housed at constant humidity (40~60%) and temperature (24 ± 2ºC) with a 12-hour light/dark cycle (lights on at 8 a.m.) and allowed free access to food and water. Handling of the animals was carried out for three days before onset of experiments. All procedures were carried out in accordance with the National Institutes of Health Guide for the Care and Use of Laboratory Animals and approved by the Institutional Animal Care and Use Committee (IACUC) at Nanjing University of Chinese Medicine.

2.2 Drug treatment

On postnatal day 28 (P28), male C57BL/6 WT mice were assigned to receive a single daily injection of cocaine hydrochloride (15 mg/kg, dissolved in saline, i.p., Qinghai Pharmaceutical, China) or saline (0.2 mL, i.p.) once daily at 10 a.m. for 14 consecutive days. From P42-P70, these mice were kept at their home cage (four mice per cage). On P71、P73 and P75, the related behavioral tests were performed. On P79, the mice were sacrificed after stimulus of elevated plus maze (EPM) procedure. The brain tissue was collected for qPCR, western blot and immunofluorescence.

2.3 Electro-acupuncture treatment

During P42 to P70, two acupuncture needles (0.16 × 7 mm, Hwato, China) were inserted gently in a depth of 2–3 mm at the acupoints of GV20 (Baihui, the midpoint between the auricular apices) and GV29 (Yintang, the midpoint between the medial ends of the two eyebrows) in each mouse, the acupoints were electric stimuli of 2/100 Hz at an intensity of 1 mA (HANS Electronic Apparatus, China) for 30 min once a day at acupoints of GV20 and GV29 in EA

mice, while at "placebo-point" (at 1 cm from base of the tail) in Sham EA (SEA) mice.

2.4 Behavioral tests

EPM, open field test (OFT), marble burying test (MBT) and novelty suppressed feeding test (NSFT) were performed to assess anxiety-like behaviors. All behavioral tests were conducted during light cycle. In the current study, four separated cohorts of the adolescent cocaine exposure mice were used to assess anxiety-like behaviors. All data were recorded and analyzed by TopScan H system (TopScan, USA). The mice were kept at their home cage until experiments.

The EPM apparatus (TopScan, Kansas City, MO, USA) consists of 4 elevated arms (52 cm above the floor) arranged in a cross pattern with two 1-cm walled arms (open arms) and two 40-cm walled arms (closed arms). Each mouse was placed in the center portion of the EPM with its head facing an open arm and allowed freely to explore the maze for 5 min. The time spent, the entries and the distance traveled in the open arms were recorded.

In OFT, mice were placed gently in the center of the open field apparatus (50 × 50 × 50 cm) individually, and the time spent and the entries into the central area (16× 16 × 16 cm) of the box and the total distance traveled in the box were recorded for 5 min with a camera positioned overhead.

In MBT, mice were placed individually in a clean cage (25 × 25 × 50 cm) with 5 cm corncob bedding. Sixteen marbles (14 mm diameter) were distributed evenly in the cages in four rows of four on top of cage bedding. Mice were left

undisturbed for 30 min, and the number of marbles buried (>50% of marble covered by bedding material) was recorded.

In NSFT, mice were placed in a square acrylic box (50 × 50 × 50 cm) with the floor covered by 3 cm of corncob bedding. Twenty-four hours before the test, all animals were food deprived. On the day of the test a single regular chow pellet was placed in a white platform located in the middle of the box. Each animal was placed in one of the apparatus corners, and the latency to start feeding in the new environment was measured with a cutoff period of 5 min. The stopwatch was immediately stopped when the mouse bit the chow, using its forepaws sitting on its haunches. After the test, all animals returned to their home cages, and the amount of food consumed in a total period of 5 min was measured.

2.5 Western blot

Total protein was extracted from claustrum in mice using RIPA lysis buffer (Beijing ComWin Biotech Co., China) according to the manufacturer's instructions. Protein samples (15 μg) was separated by 10% SDS–PAGE, 12% SDS–PAGE and electrophoretically transferred onto PVDF membranes. The transferred membranes were blocked with 5% non-fat dry milk or 5% BCA and 0.1% Tween 20 in 10 mM Tris–HCl (TBST buffer, pH 7.5) for 1.5 h at room temperature, then subsequently incubated with the following primary antibodies: D1R (1:1000, Rabbit, RRID:AB_10598308, Proteintech, USA), D2R (1:1000, Rabbit, ER1907-70, Hua An Biotechnology Company, China), D3R (1:1000, Mouse, ab155098, Abcam, UK), $ERK_{1/2}$ (1:1000, Rabbit, BM4326, Boster, China), p-$ERK_{1/2}$ (1:1000, Rabbit, BM4326, Boster, China), CREB (1:1000, Rabbit, RRID:AB_10699020, Cell Signaling Technology, USA), p-CREB

(1:1000, Rabbit, RRID:AB_2561044, Cell Signaling Technology, USA), c-Fos (1:2000, Rabbit, RRID:AB_2247211, Cell Signaling Technology, USA), BDNF (1:1000, Mouse, RRID:AB_2881675, Proteintech, USA). The next day, the membranes were washed three times in Tris-buffered saline with Tween 20 (TBS-T) and incubated with horseradish peroxidase (HRP)-conjugated secondary antibody goat anti-rabbit or goat anti mouse (1:5000, Beijing ComWin Biotech Co., China) at room temperature for 1 h. The blots were visualized by the ECL kit (Beyotime, China) and the signal was visualized by imaging system (Tanon-5200, Shanghai, China). The blots were washed with stripping buffer (Beyotime Institute of Biotechnology) to allow reprobing with other antibodies. In this study, GAPDH or β-actin was used as the loading control. Values for target protein levels were calculated using Image J software (NIH, USA). The relative level of each protein expression (blot volume) was normalized to GAPDH or β-actin.

2.6 RNA extraction and quantitative real-time PCR

Mice were decapitated 45 min following EPM behavioral tests on P79. Claustrum were collected immediately. Total RNA was extracted from the middle of claustrum using FastPure Cell/Tissue Total RNA Isolation Kit (Vazyme, China), according to the manufacturer's instructions. All samples were tested for concentration and purified using a 4200 TapeStation (Agilent Technologies, Santa Clara, USA). After RNA extraction, the amount of RNA was normalized across samples, and cDNA was created using iScript (1708891, Bio-Rad, Hercules, USA). Actin was used as the internal control. The primers of *D1R, D2R*, *D3R* and Actin were as follows: *D1R* (forward, ATGGCTCCTAACACTTCTACCA; reverse,

GGGTATTCCCTAAGAGAGTGGAC); *D2R* (forward, ACCTGTCCTGGTACGATGATG; reverse, GCATGGCATAGTAGTTGTAGTGG); *D3R* (forward, AGACAACATGGAGAGCTGAAACGCT; reverse, TTCAGGGCTGTGGATAACCTGCC); Actin (forward, GGCTGTATTCCCCTCCATCG; reverse, CCAGTTGGTAACAATGCCATGT). *D1R*, *D2R* and *D3R* mRNA levels were normalized to Actin mRNA levels. The relative mRNA level was calculated by the comparative CT method ($2^{-\Delta\Delta Ct}$).

2.7 Immunofluorescence

Mice brains were collected within 90 min after EPM procedure and perfused with 4% paraformaldehyde (PFA). The coronal brain sections (30 μm) were cut on a cryostat (Leica, Germany). The sections were incubated in 0.3% (v/v) Triton X-100 for 0.5 h, blocked with 5% donkey serum for 1.5 h at room temperature, and incubated overnight at 4°C with the following primary antibodies: rabbit anti-c-Fos (1:2000, RRID: AB_2247211, Cell Signalling Technology, USA) , mouse anti-NeuN (1:800, RRID: AB_2298772, Millipore, USA), mouse anti-GAD67 (1:800, RRID: AB_2278725, Millipore, USA), mouse anti-PV (1:250, BM1339, Boster Biotechnology, China), mouse anti-SOM (1:50, RRID: AB_2271061, Santa Cruz, USA) and mouse anti-CaMKIIα (1:100, RRID: AB_626789, Santa Cruz, USA), followed by the corresponding fluorophore-conjugated secondary antibodies for 1 h at room temperature. The following secondary antibodies were used here: Alexa Fluor 555-labeled donkey anti-rabbit secondary antibody (1:500, RRID: AB_162543, Invitrogen, USA), Alexa Fluor 488-labeled donkey anti-mouse secondary antibody (1:500, RRID: AB_141607, Invitrogen, USA). Fluorescence signals were visualized using a

Leica DM6B upright digital research microscope (Leica, Germany) or Leica TCS SP8 (Leica, Germany).

2.8 Local administration of SCH-23390 in claustrum

The cannula (O.D. 0.41 mm, C.C 3.0 mm, Cat 62004, RWD, China) were planted into claustrum (AP + 0.75 mm, ML ± 3.30 mm, DV – 2.50 mm) of ACE mice on P64 before anxiety-like behaviors test. After surgery, mice were maintained at home cage about 1 week. From P71, mice were subjected to EPM, OFT, NSFT. The D1 receptor antagonist R(+)-7-chloro-8-hydroxy-3-methyl-1-phenyl-2,3,4,5-tetrahydro-1H-3-benzazepine hydrochloride (SCH-23390, Selleck chemicals, China) was dissolved in 0.9% saline and stored -80°C. A volume of 70 nL of SCH-23390 were bilaterally injected into claustrum at a rate of 10 nL/min at 20 min prior to behavioral tests.

2.9 Specific knockdown of D1R on CaMKII-positive neurons of claustrum

On P50, mice were anesthetized with 2% isoflurane in oxygen, and were fixed in a stereotactic frame (RWD, Shenzhen, China). A heating pad was used to maintain the core body temperature of the mice at 36°C. The coordinates of claustrum were defined as AP + 0.62 mm, ML ± 3.05 mm, DV –3.50 mm. A volume of 70 nL virus of *CaMKIIap-EGFP-MIR155(shDrd1)-SV40 PolyA* (KD group, Titer: 8.89E+13v.g/ml, GeneChem, Shanghai, China) and *CaMKIIap-EGFP-MIR155(MCS)-SV40 PolyA* (Ctrl group, Titer: 1E+13v.g/ml, GeneChem, Shanghai, China) were injected bilaterally into claustrum at a rate of 10 nL/min. After surgery, mice were kept at home-cage about 3 weeks.

2.10 Statistical analysis

Statistical analysis was carried out using GraphPad Prism 8.0.2 software. Data are presented as the Mean ± SEM. The MBT results was analyzed by Two-Way ANOVA followed by Šídák's multiple comparisons test. Other data was analyzed by unpaired t-tests. Statistical significance was set as $p < 0.05$.

3. Results

3.1 ACE enhances anxiety with evoked claustrum and D1R^{CaMKII} in mice of adulthood

To examine anxiety-like behaviors following ACE, mice were subjected to behavioral tests of EPM, OFT and MBT in their adulthood (Figure 1A). As shown in Figure 1B, ACE mice of adulthood exhibited less time spent (n = 24, t = 2.292, p = 0.0319) and less entries (n = 24, t = 2.120, p = 0.0455) into the open arms, but similar distances traveled in open arms of the EPM apparatus (n = 24, t = 1.497, p = 0.1486) than those of adolescent saline exposure (ASE) mice of adulthood. During the OFT (Figure 1C), ACE mice spent less time (n = 24, t = 2.308, p = 0.0308) in the central area of box, while had similar entries (n = 24, t = 1.488, p = 0.1509) into the central area and total distances traveled (n = 24, t = 0.008965, p = 0.9929) in the OFT box than ASE controls. In the MBT, the buried beads by ACE mice had no significant difference at each time point (n = 24, $F_{(6,132)}$ = 0.3929，p = 0.8826) and in total (n = 24, t = 0.8578, p = 0.4003) when compared to ASE controls (Figure 1D).

The c-Fos and CaMKII were used as markers to detect the neuronal activity and glutamatergic neurons, respectively. The total protein level of c-Fos (n = 6, t = 2.811, p = 0.0483) was higher in ACE than in ASE mice of adulthood (Figure 1E). Both the percentage (n = 11, t = 2.466, p = 0.0358) and number (n = 11, t = 3.106, p = 0.0126) of c-Fos-positive & CaMKII-positive neurons were higher

in ACE mice than those in ASE mice of adulthood (Figure 1F).

On CaMKII-positive neurons, the expression of D1R ($D1R^{CaMKII}$) was much higher (n = 6, t = 3.177, p = 0.0336) in ACE than in ASE mice of adulthood (Figure 1G). The total levels of mRNA (Figure 1H) and protein (Figure 1I) of claustral D1R (mRNA, n = 9, t = 2.583, p = 0.0363; protein, n = 6, t = 7.389, p = 0.0018) was higher, but not that of D2R (mRNA, n = 11, t = 0.2676, p = 0.7950; protein, n = 6, t = 0.1621, p = 0.8791) and D3R (mRNA, n = 11, t = 0.3458, p = 0.7374; protein, n = 6, t = 1.159, p = 0.2035) in ACE than in ASE mice of adulthood. In parallel, the protein levels of p-$ERK_{1/2}$ (n = 6, t = 4.905, p = 0.0080), ratio of p-$ERK_{1/2}$ to $ERK_{1/2}$ (n = 6, t = 3.239, p = 0.0317), p-CREB (n = 6, t = 5.871, p = 0.0042), p-CREB/ CREB (n = 6, t = 3.502, p = 0.0248) and BDNF (n = 6, t = 2.940, p = 0.0424) were higher in ACE group mice than controls, but that of $ERK_{1/2}$ (n = 6, t = 0.9475, p = 0.3970) and CREB (n = 6, t = 0.4336, p = 0.6869) had no significant difference between ACE and ASE mice of adulthood (Figure 1J, 1K).

Figure 1

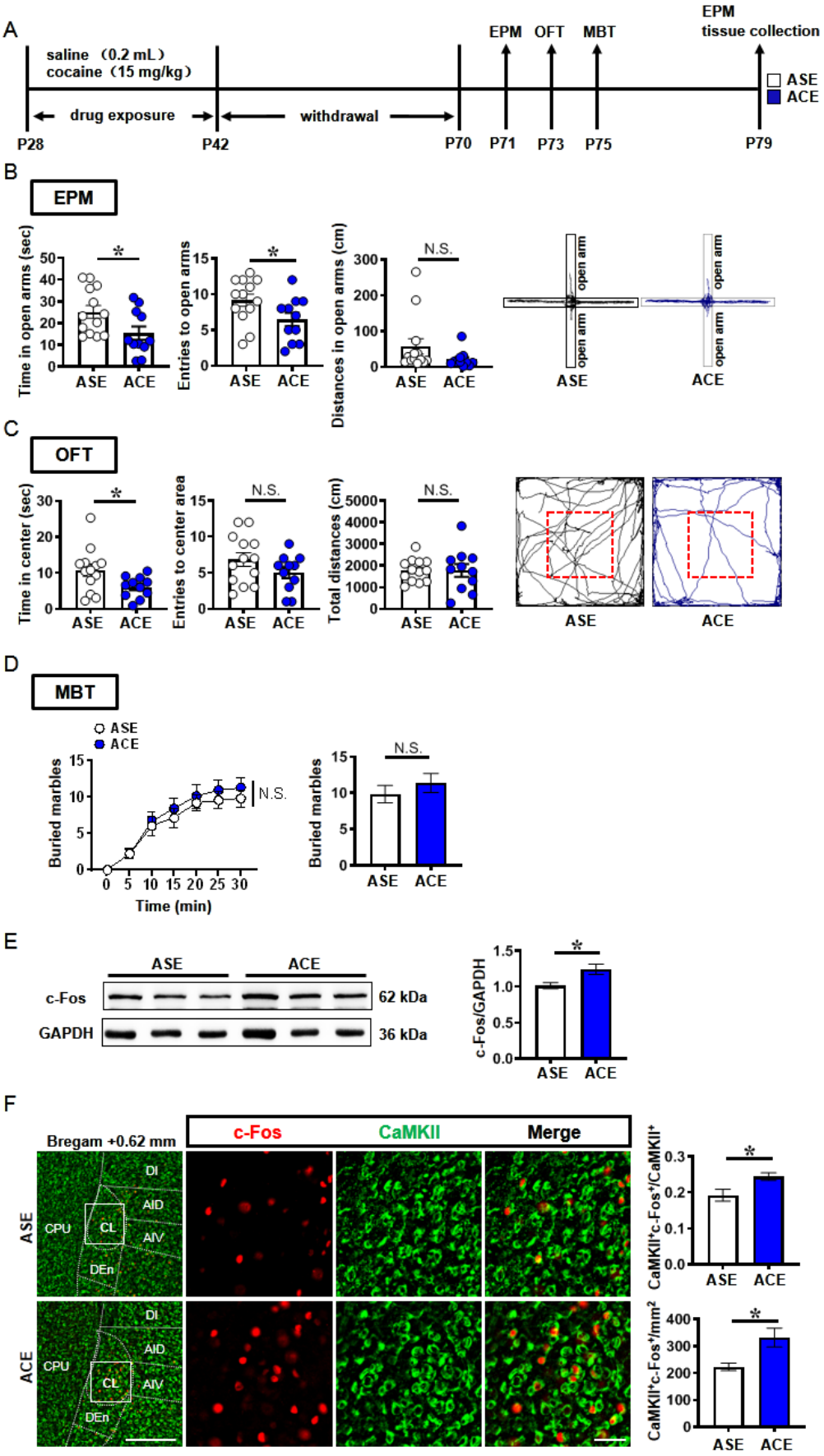
A
saline (0.2 mL)
cocaine (15 mg/kg)
drug exposure
withdrawal
P28
P42
P70
P71
P73
P75
P79
EPM
OFT
MBT
EPM
tissue collection
ASE
ACE
B
EPM
Time in open arms (sec)
Entries to open arms
Distances in open arms (cm)
N.S.
open arm
open arm
open arm
open arm
ASE
ACE
C
OFT
Time in center (sec)
Entries to center area
Total distances (cm)
N.S.
N.S.
ASE
ACE
D
MBT
ASE
ACE
Buried marbles
N.S.
Time (min)
Buried marbles
N.S.
ASE
ACE
E
ASE
ACE
c-Fos
GAPDH
62 kDa
36 kDa
c-Fos/GAPDH
ASE
ACE
F
Bregam +0.62 mm
c-Fos
CaMKII
Merge
ASE
ACE
CPU
CL
DI
AID
AIV
DEn
CaMKII+c-Fos+/CaMKII+
CaMKII+c-Fos+/mm2
ASE
ACE

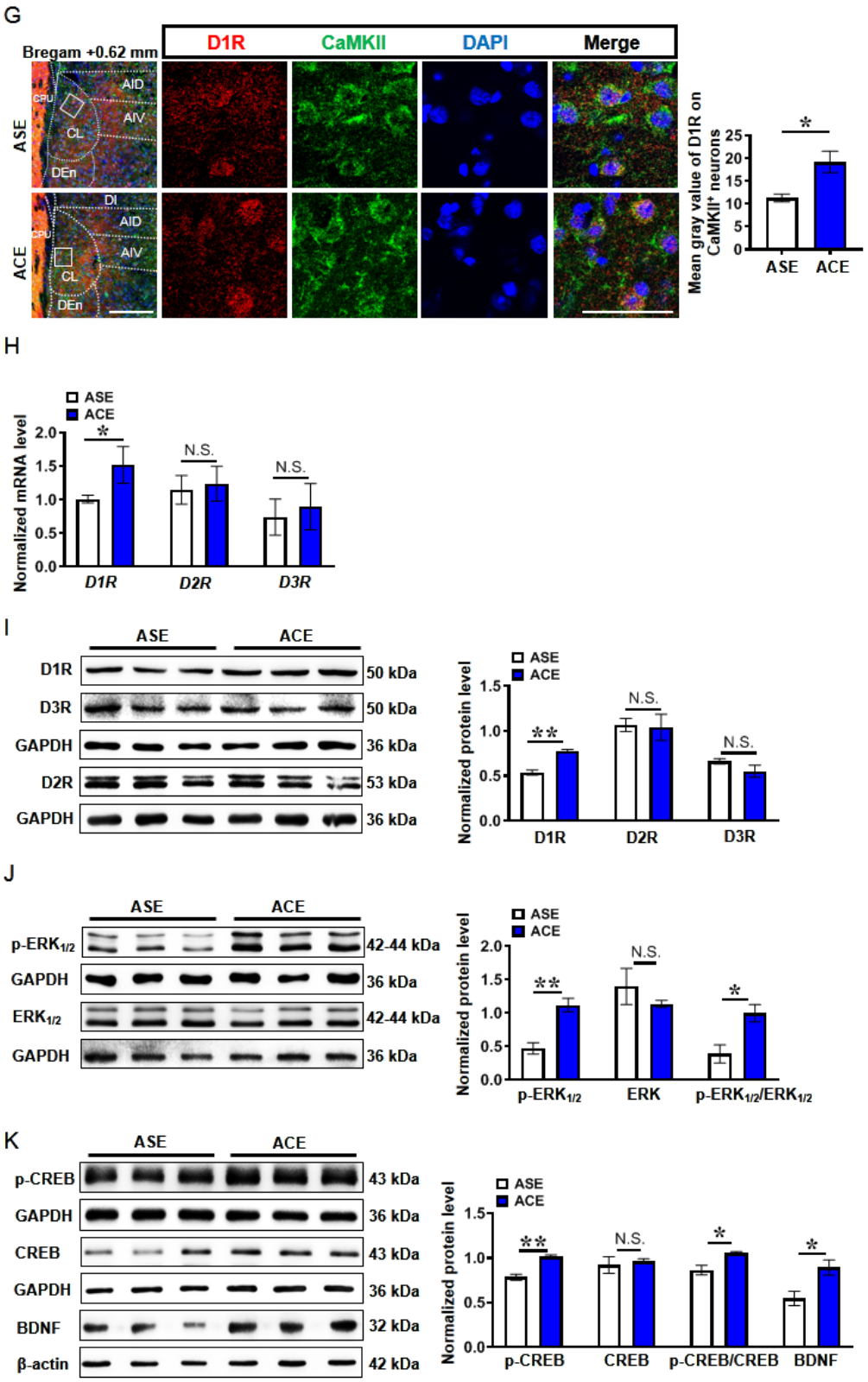

Figure 1. ACE enhances anxiety with evoked claustrum and D1R^{CaMKII} in mice of adulthood. A, Experimental timeline. **B**, EPM test. **C**, OFT. **D**, MBT. **E**, Total protein levels of c-Fos. **F**, The percentage and number of c-Fos-positive

& CaMKII-positive neurons. Scale bar, 300 μm/50 μm. **G,** The expression of $D1R^{CaMKII}$. Scale bar, 200 μm/50 μm. **H**, The mRNA levels of *D1R, D2R and D3R*. **I,** The protein levels of D1R, D2R and D3R. **J,** Levels of p-$ERK_{1/2}$ and $ERK_{1/2}$. **K,** Levels of p-CREB, CREB and BDNF. ASE, adolescent saline exposure; ACE, adolescent cocaine exposure; CL, claustrum. N.S., $p > 0.05$, *, $p < 0.05$, **, $p < 0.01$ vs ASE.

3.2 Blocking D1R within claustrum suppresses ACE-increased anxiety and claustrum activation in mice of adulthood

To evaluate the role of claustral D1R in ACE-induced anxiety, the selective D1R antagonist SCH-23390 was bilaterally injected into local claustrum 20 min prior to the tests of EPM, OFT and NSFT (Figure 2A). Compared with vehicle-treated mice, local SCH-23390 treatment significantly enhanced the time spent in open arms (n = 19, $t = 2.322$, $p = 0.0329$), and did not affect the entries into the open arms (n = 19, $t = 1.085$, $p = 0.2930$) and the distances traveled in open arms of EPM apparatus (n = 19, $t = 0.5363$, $p = 0.5987$) in ACE mice of adulthood (Figure 2B). SCH-23390 treatment had no influence in the time spent (n = 19, $t = 1.688$, $p = 0.1096$), the entries (n = 19, $t = 1.105$, $p = 0.2847$) in the central area, and the total distances traveled by ACE mice (n = 19, $t = 1.676$, $p = 0.1121$) in the OFT box, when compared with the vehicle-treated mice (Figure 2C). Similarly, there is no difference on the latency (n = 19, $t = 0.6239$, $p = 0.5410$) and intake (n = 19, $t = 0.9492$, $p = 0.3558$) of feeding in the NSFT between vehicle-treated and SCH-23390-treated ACE mice (Figure 2D).

As shown in Figure 2E, local SCH-23390 treatment significantly attenuated the number of c-Fos-positive neurons (n = 12, $t = 3.097$, $p = 0.0113$), when compared with vehicle-treated mice.

Figure 2

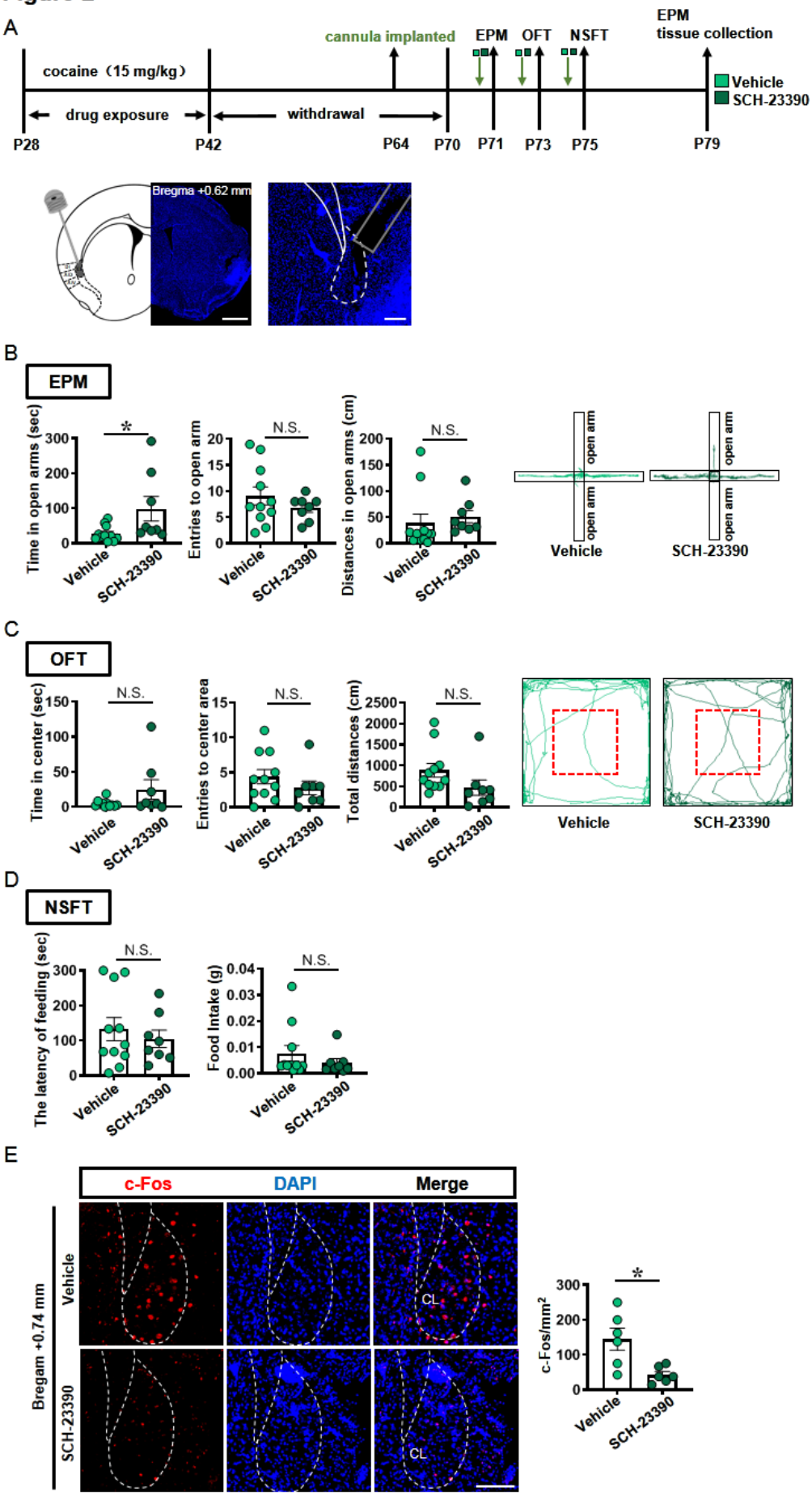
A
cannula implanted
EPM
OFT
NSFT
EPM
tissue collection
cocaine（15 mg/kg）
Vehicle
SCH-23390
drug exposure
withdrawal
P28
P42
P64
P70
P71
P73
P75
P79
Bregma +0.62 mm
B
EPM
Time in open arms (sec)
Entries to open arm
Distances in open arms (cm)
N.S.
*
Vehicle
SCH-23390
open arm
C
OFT
Time in center (sec)
Entries to center area
Total distances (cm)
D
NSFT
The latency of feeding (sec)
Food Intake (g)
E
c-Fos
DAPI
Merge
Bregam +0.74 mm
CL
c-Fos/mm²

Figure 2. Blocking D1R within claustrum suppresses ACE-increased anxiety and claustrum activation in mice of adulthood. A, Experimental timeline and local injections of SCH-23390 into claustrum. Scale bar, 400/100 μm. **B**, EPM test. **C**, OFT. **D**, NSFT. **E,** The number of c-Fos-positive neurons. Scale bar, 100 μm. Vehicle, vehicle-treated ACE mice; SCH-23390, SCH-23390-treated ACE mice; CL, claustrum. N.S., $p > 0.05$, *, $p < 0.05$, **, $p < 0.01$ vs Vehicle.

3.3 Knocking-down D1R^{CaMKII} of claustrum suppresses ACE-increased anxiety and claustrum activation in mice of adulthood

Specific knockdown of D1R^{CaMKII} was performed in ACE mice of adulthood (Figure 3A). Adeno-associated virus of either *CaMKIIap-EGFP-MIR155(shDrd1)-SV40 PolyA* (ACE$_{KD}$) or *CaMKIIap-EGFP-MIR155(MCS)-SV40 PolyA* (ACE$_{Ctrl}$) was bilaterally infused into clautrum, and about 55% CaMKII-positive neurons within clautrum were transfected with virus (Figure 3B). Compared with ACE$_{Ctrl}$ mice, the levels of D1R protein (n = 6, $t = 3.465$, $p = 0.0257$, Figure 3C) was decreased in CL of ACE$_{KD}$ mice.

ACE$_{KD}$ mice exhibited more time spent (n = 16, $t = 2.152$, $p = 0.0493$), and did not affect the entries into the open arms (n = 16, $t = 1.134$, $p = 0.2759$), and similar distance traveled (n = 16, $t = 1.831$, $p = 0.0885$) in the EPM apparatus, when compared with ACE$_{Ctrl}$ mice (Figure 3D). There were no differences on the time spent in central area (n = 16, $t = 1.500$, $p = 0.1559$), the entries (n = 16, $t = 0.1574$, $p = 0.8772$) in the central area, the total distances traveled by ACE mice (n = 16, $t = 0.1926$, $p = 0.8500$) in the OFT box (Figure 3E). Moreover, the latency (n = 16, $t = 0.02965$, $p = 0.9768$) and intake (n = 16, $t = 1.088$, $p = 0.2950$) of feeding did not change in the NSFT (Figure 3F) between ACE$_{KD}$ and

ACE_{Ctrl} mice. In parallel, the percentage of c-Fos-positive neurons in EGFP-transfected neurons (n = 6, t = 3.207, p = 0.0327) and the mean gray value of c-Fos in EGFP-transfected neurons (n = 6, t = 3.006, p = 0.0397) were much lower in ACE_{KD} mice than that in ACE_{Ctrl} mice (Figure 3G).

Figure 3

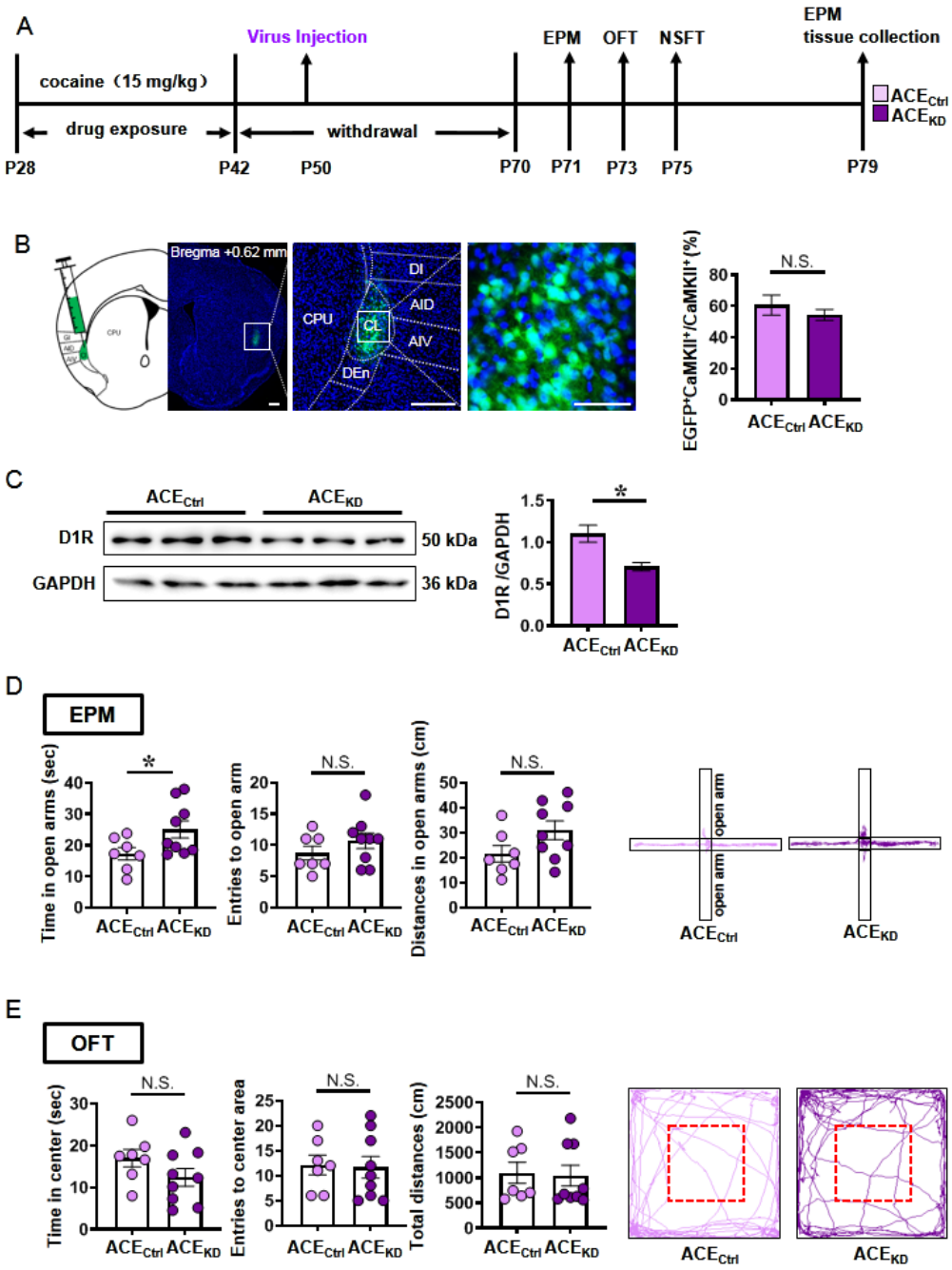

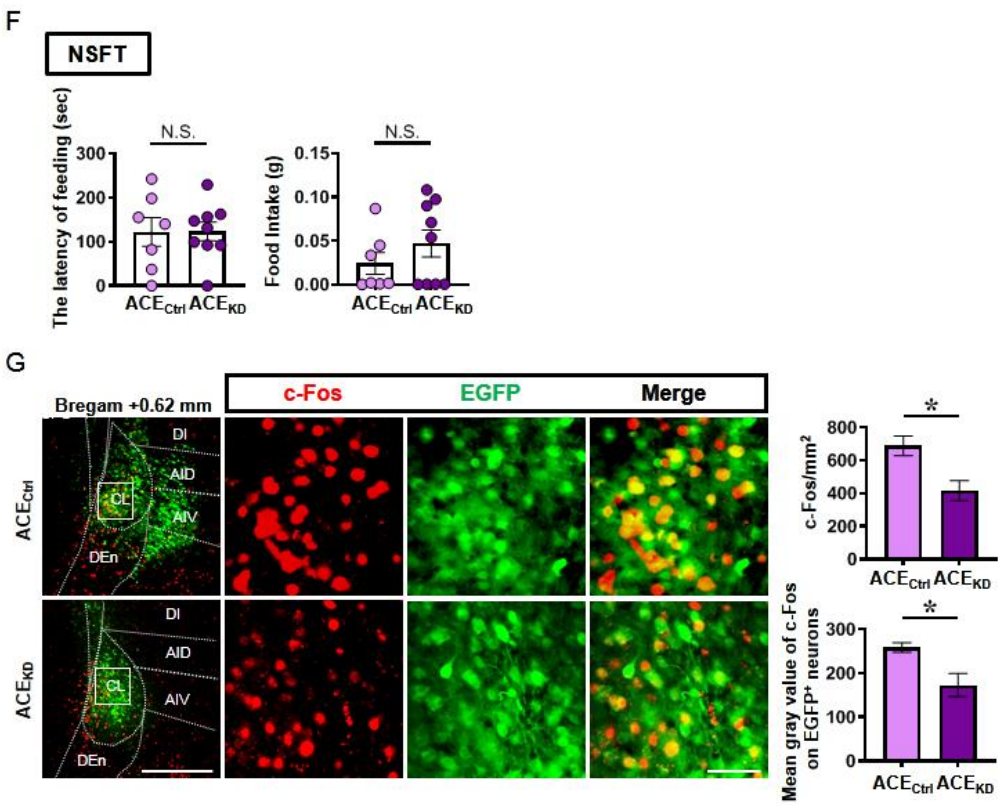

Figure 3. Knocking-down D1R^{CaMKII} of claustrum suppresses ACE-increased anxiety and claustrum activation in mice of adulthood. A, Experimental design and timeline. **B**, Local injections of virus into claustrum. Scale bar, 300 μm. **C**, The D1R protein level. **D**, EPM test. **E**, OFT. **F**, NSFT. **G**, The percentage of c-Fos-positive neurons in EGFP-transfected neurons and the mean gray value of c-Fos in EGFP-transfected neurons. Scale bar, 400 μm/50 μm. ACE, adolescent cocaine exposure; ACE_{Ctrl}, ACE mice injected with control virus; ACE_{KD}, ACE mice injected with knockdown virus; CL, claustrum. N.S., $p > 0.05$, *, $p < 0.05$, **, $p < 0.01$ vs ACE_{Ctrl}.

3.4 EA treatment rescues ACE-increased anxiety in mice of adulthood by suppressing claustrum activation and D1R^{CaMKII}

EA treatments at acupoints of GV20 and GV29 during P42-P70 were carried out in ACE mice (ACE_{EA}), and placebo acupoints were used as sham EA

treatment (ACE_{SEA}) (Figure 4A, 4B). Compared with ACE_{SEA} mice, ACE_{EA} mice spent more time (n = 23, t = 2.084, p = 0.0496), similar entries into the open arms (n = 23, t = 1.536, p = 0.1394) and similar distances traveled in open arms of the EPM apparatus (n = 23, t = 1.186, p = 0.0837, Figure 4C). There were no differences in the time spent (n = 23, t = 0.1918, p = 0.8498), the entries (n = 23, t = 0.08086, p = 0.9363) into the central area and the total distances traveled (n = 23, t = 0.3799, p = 0.7078) in the OFT box between ACE_{EA} and ACE_{SEA} mice (Figure 4D). In the NSFT (Figure 4E), ACE_{EA} mice intake more food (n = 23, t = 2.532, p = 0.0194), and spent similar latency of feeding (n = 23, t = 0.6190, p = 0.5426), when compared with ACE_{SEA} mice.

Compared with ACE_{SEA} mice, both the percentage (n = 12, t = 4.246, p = 0.0017) and the number (n = 12, t = 3.076, p = 0.0117) of c-Fos-positive & CaMKII-positive neurons were much lower in ACE_{EA} mice (Figure 4F). In parallel, both levels of total D1R protein in CL (n = 6, t = 4.396, p = 0.0117, Figure 4G) and $D1R^{CaMKII}$ staining (n = 6, t = 4.874, p = 0.0082, Figure 4H) were lower in ACE_{EA} mice than that in ACE_{SEA} mice.

As shown in Figure 4I-J, there were no differences on protein levels p-$ERK_{1/2}$ (n = 6, t = 0.2242, p = 0.8336), $ERK_{1/2}$ (n = 6, t = 0.7388, p = 0.5010), CREB (n = 6, t = 0.9656 p = 0.3889) and ratio of p-$ERK_{1/2}$ to $ERK_{1/2}$ (n = 6, t = 0.3008, p = 0.7786) in claustrum between ACE_{EA} and ACE_{SEA} mice. While, the levels of p-CREB (n = 6, t = 4.464, p = 0.0111), BDNF (n = 6, t = 2.957, p = 0.0417) and radio of p-CREB to CREB (n = 6, t = 3.191, p = 0.0332) were lower in ACE_{EA} mice, when compared with ACE_{SEA} mice.

Figure 4

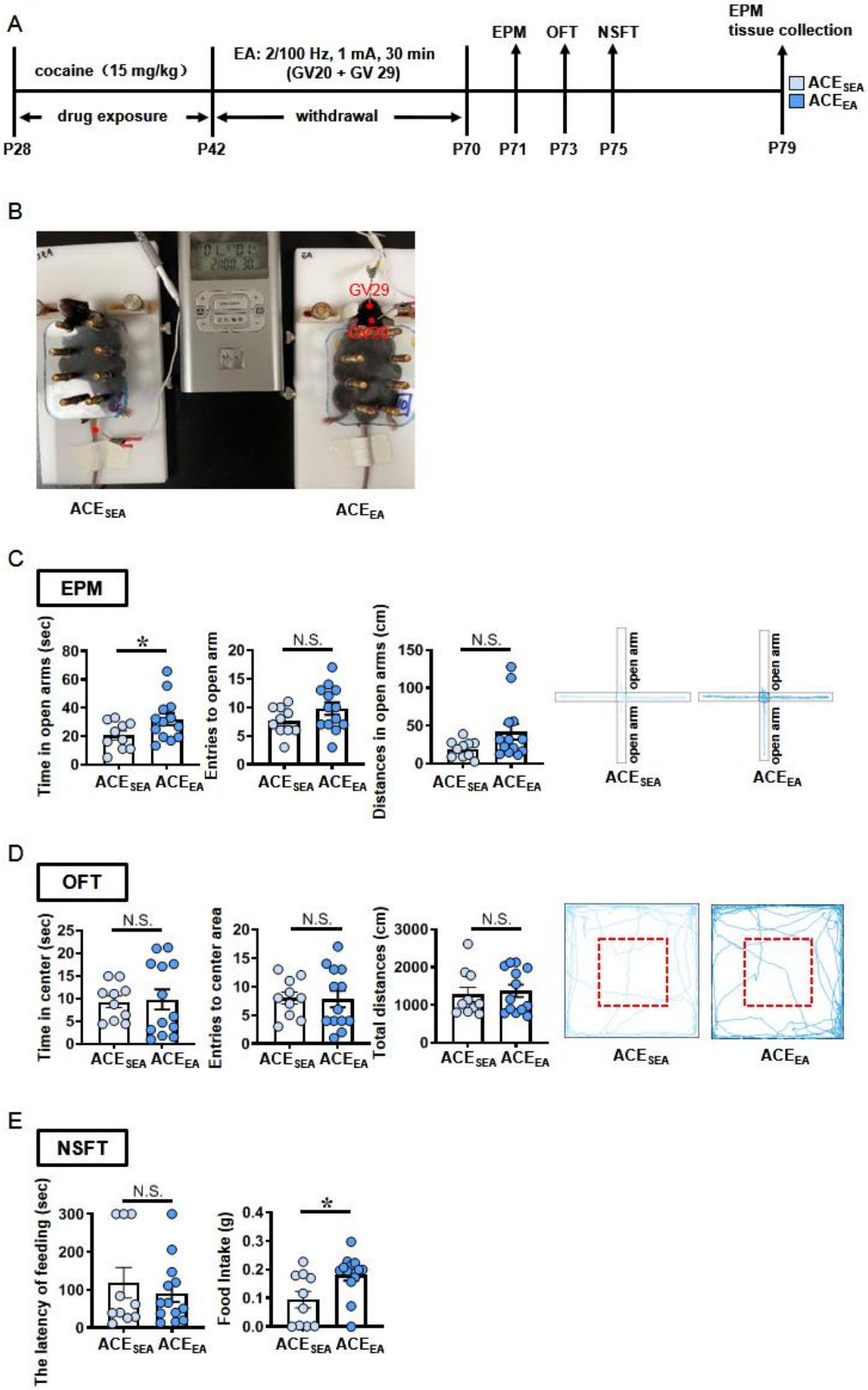
A
cocaine（15 mg/kg）
EA: 2/100 Hz, 1 mA, 30 min
(GV20 + GV 29)
EPM
OFT
NSFT
EPM
tissue collection
ACE$_{SEA}$
ACE$_{EA}$
drug exposure
withdrawal
P28
P42
P70
P71
P73
P75
P79
B
GV29
GV20
ACE$_{SEA}$
ACE$_{EA}$
C
EPM
Time in open arms (sec)
Entries to open arm
Distances in open arms (cm)
N.S.
*
open arm
ACE$_{SEA}$
ACE$_{EA}$
D
OFT
Time in center (sec)
Entries to center area
Total distances (cm)
N.S.
ACE$_{SEA}$
ACE$_{EA}$
E
NSFT
The latency of feeding (sec)
Food Intake (g)
N.S.
*
ACE$_{SEA}$
ACE$_{EA}$

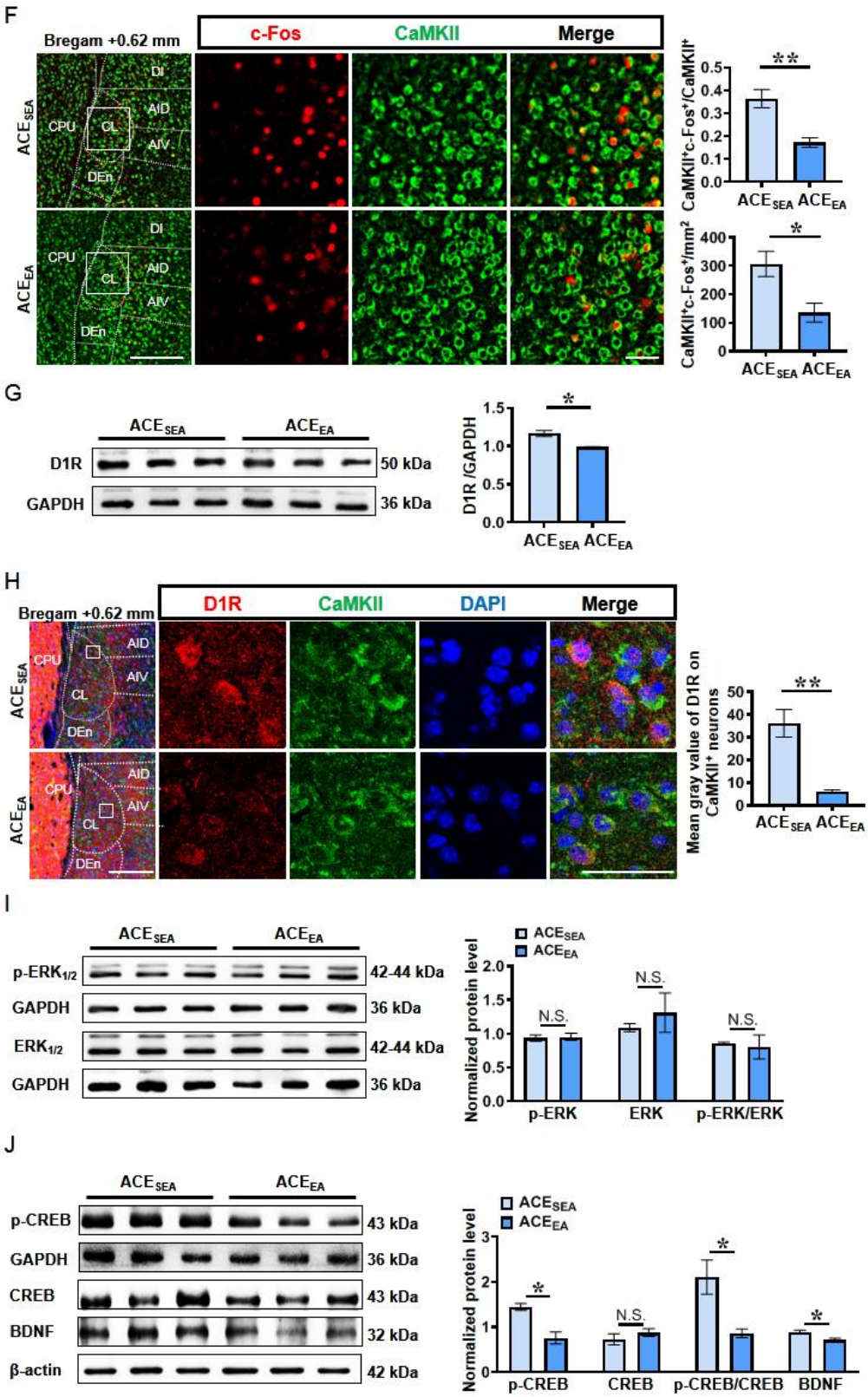

Figure 4. EA treatment rescues ACE-increased anxiety in mice of adulthood by suppressing claustrum activation and D1R^{CaMKII}. A,

Experimental design and timeline. **B**, Schematic diagram of EA and SEA treatments in mice. **C**, EPM test. **D**, OFT. **E**, NSFT. **F**, The percentage and number of c-Fos-positive & CaMKII-positive neurons. Scale bar, 300 μm/50 μm. **G**, The D1R protein level. **H**, The staining of $D1R^{CaMKII}$. Scale bar, 200 μm/50 μm. **I**, Levels of p-$ERK_{1/2}$ and $ERK_{1/2}$. **J**, Levels of p-CREB, CREB and BDNF. ACE_{SEA}, sham electro-acupuncture-treated ACE mice; ACE_{EA}: electro-acupuncture (GV 20 and GV 29)-treated ACE mice; CL, claustrum. N.S., $p > 0.05$, *, $p < 0.05$, **, $p < 0.01$ vs ACE_{SEA}.

4. Discussion

Adolescent cocaine exposure (ACE) produces obvious anxiety in mice of adulthood. In parallel, ACE evokes CaMKII-positive neurons in claustrum and increases D1R expression on CaMKII-positive neurons ($D1R^{CaMKII}$). Blocking D1R or knocking-down $D1R^{CaMKII}$ within claustrum efficiently rescues ACE-increased claustrum activation and $D1R^{CaMKII}$, and ultimately suppresses ACE-induced anxiety in mice. EA at acupoints of Baihui (GV 20) and Yintang (GV 29) alleviates ACE-induce anxiety by targeting claustral $D1R^{CaMKII}$ in mice of adulthood (Figure 5).

Figure 5

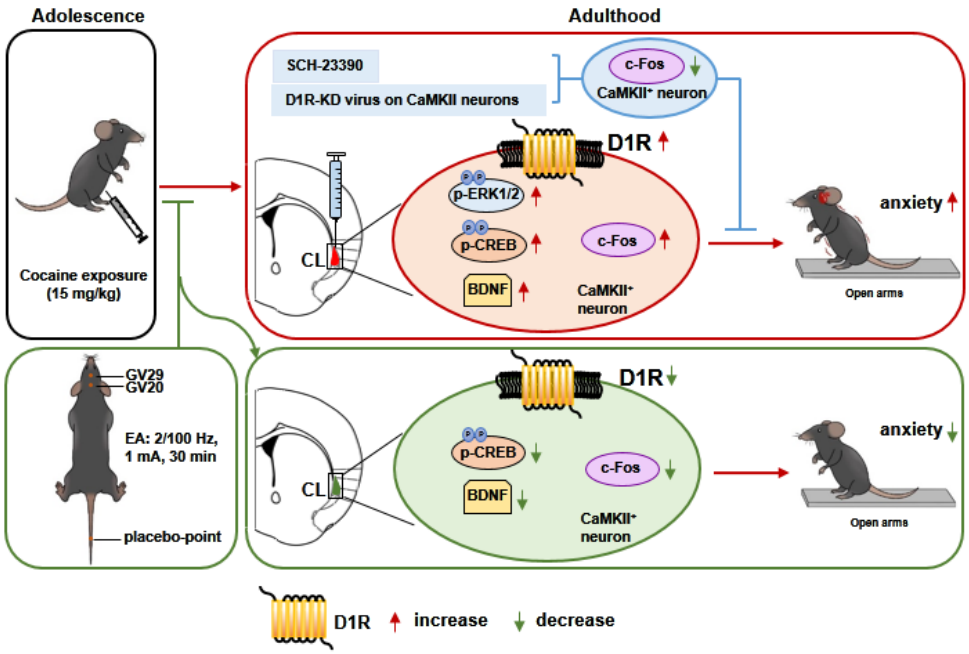

Figure 5. Schematic summary of present study. Adolescent cocaine exposure (ACE) enhances anxiety-like behaviors in mice of adult, accompanied with triggered activation of CaMKII-positive neurons and more dopamine receptor 1 (D1R) on CaMKII-positive neurons ($D1R^{CaMKII}$) in claustrum. Either blocking D1R with SCH23390 or knocking-down $D1R^{CaMKII}$ with virus in the claustrum efficiently reduce claustrum activation, and ultimately suppresses ACE-induced anxiety in mice. By targeting claustral $D1R^{CaMKII}$, electro-acupuncture (EA) at acupoints of GV20 and GV29 rescues ACE-increased anxiety in mice of adulthood. In the process, the p-CREB and BDNF may be the potential subsequent signals to $D1R^{CaMKII}$.

Consistent with human and animal studies on ACE [7,29,32,33], including ours, here we found that ACE mice exhibited more anxiety in their adulthood. Further, we found that CaMKII-positive neurons in claustrum seem to be involved in the process. Recently, Niu et.al [24] report that claustrum is crucial

encoding stress-induced anxiety, as indicated by attenuation of stress-induced anxiety with silencing CaMKII-positive neurons in claustrum. Claustrum receives inputs and sends back axonal outputs to the prefrontal cortex (PFC), a critical region coding cocaine-related anxiety [34,35]. In our previous study, we found that ACE altered the function of local circuit from GABAergic interneuron to pyramidal neurons in mPFC, which mediates ACE-increased anxiety in adult mice [7]. Due to the robust communications between mPFC and claustrum, ACE-triggered claustrum should contribute to the anxiety in mice of adulthood. Firstly, we explored the potential molecules that underlie the evoked claustrum by ACE. A recent study by Terem et al. [23] found that D1R-positive ($D1R^{+}$) neurons in claustrum, especially those connected with PFC are required for acquisition and reinstatement of cocaine preference. They focus the cell subgroups of $D1R^{+}$ and $D1R^{-}$ in cocaine-preferred behaviors. Here, our findings show that it is $D1R^{CAMKII}$ that were elevated by ACE in claustrum of adult mice, and we focus on the role of D1R in activation of CaMKII-positive neurons and ACE-related anxiety. Moreover, locally blocking D1R or knocking-down $D1R^{CaMKII}$ in claustrum reduced ACE-evoked claustrum and subsequent anxiety. These findings indicate that activity of claustrum CaMKII-positive neurons encodes ACE-increased anxiety, which is mediated at least partially by $D1R^{CaMKII}$. In other D1R-rich brain regions, such as PFC and hippocampus, cocaine abuse could alter p-ERK [36], p-CREB [37] and BDNF [38,39]. Here, we found that protein levels of p-ERK, p-CREB and BDNF were significantly increased in claustrum of ACE mice, implying that they are potential downstream signals for claustral $D1R^{CaMKII}$ in the process of ACE-induced anxiety.

At present, neither D1R antagonists nor specific virus-regulated D1R could be clinically used to treat emotional disorders such as ACE-induced anxiety in humans. EA has been widely applied in management of substance abuse, especially for drugs-caused withdrawal symptoms, including anxiety [28,29,40]. Shao et al [41] reported that EA at Zusanli (ST36) and Kunlun (BL60) could reduce anxiety-like behaviors in animals by suppressing neuropeptide Y in anterior cingulate cortex. Wu et al. [42] found that EA at ST36 and Sanyinjiao (SP6) alleviated anxiety by activating D1R or antagonizing D2R in the basolateral amygdala. Previously, we found that EA with a stimulus of a mixed frequency of 2/100 Hz could alleviate ACE-induced anxiety in mice [29]. With the findings of claustrum here, we speculated that claustral $D1R^{CaMKII}$ might be one pharmacological targets of EA treatment. As expected, we found that EA at acupoints of GV20 and GV29 reversed ACE-enhanced claustrum activation by suppressing claustral $D1R^{CaMKII}$, which ultimately ameliorated ACE-induced anxiety.

Collectively, our findings identified a novel role of claustrum in ACE-induced anxiety, and put new insight into the function of claustral $D1R^{CaMKII}$. By targeting claustral $D1R^{CaMKII}$, EA obviously alleviates ACE-induced anxiety in mice of adulthood.

Author contribution

Chen L and Fan Y have equal contribution to the manuscript. Chen L, Fan Y, Liu Z and Zhao Z performed behavioral tests, morphological tests and virus-related experiment. Guo H, Du D, Pan W, Wei X and Nie J assist the experiment. Fan Y, Ge F and Ding J performed data analysis. Guan X and Fan Y wrote the

manuscript. Kim HY edited the manuscript. Guan X developed the overall concept.

Fundings

This work is supported by National Natural Science Foundation of China (82211540400, 82271531 and 82071495), Natural Science Foundation of Jiangsu Province, China (BK20201398) and Natural Science Foundation of the Higher Education Institutions of Jiangsu Province, China (21KJB360007).

Competing interests

The authors have no conflict of interests to declare.

Data availability statement

The data that support the findings of this study are available from the corresponding author upon reasonable request.

Reference

1 Laviola G, Adriani W, Terranova ML, Gerra G. Psychobiological risk factors for vulnerability to psychostimulants in human adolescents and animal models. Neuroscience and biobehavioral reviews. 1999;23(7):993-1010.

2 Chambers RA, Taylor JR, Potenza MN. Developmental neurocircuitry of motivation in adolescence: a critical period of addiction vulnerability. The American journal of psychiatry. 2003;160(6):1041-52.

3 Moss HB, Chen CM, Yi HY. Early adolescent patterns of alcohol, cigarettes, and marijuana polysubstance use and young adult substance use outcomes in a nationally representative sample. Drug and alcohol dependence. 2014;136:51-62.

4 Rutherford HJ, Mayes LC, Potenza MN. Neurobiology of adolescent substance use disorders: implications for prevention and treatment. Child and adolescent psychiatric clinics of North America. 2010;19(3):479-92.

5 Stopponi S, Soverchia L, Ubaldi M, Cippitelli A, Serpelloni G, Ciccocioppo R. Chronic THC during adolescence increases the vulnerability to stress-induced relapse to heroin seeking in adult rats. European neuropsychopharmacology : the journal of the European College of Neuropsychopharmacology. 2014;24(7):1037-45.

6 Erb S. Evaluation of the relationship between anxiety during withdrawal and stress-induced reinstatement of cocaine seeking. Progress in neuro-psychopharmacology & biological psychiatry. 2010;34(5):798-807.

7 Shi P, Nie J, Liu H, Li Y, Lu X, Shen X, et al. Adolescent cocaine exposure enhances the GABAergic transmission in the prelimbic cortex of adult mice. FASEB journal : official publication of the Federation of American Societies for Experimental Biology. 2019;33(7):8614-22.

8 Zhu W, Ge X, Gao P, Li M, Guan Y, Guan X. Adolescent cocaine exposure induces prolonged synaptic modifications in medial prefrontal cortex of adult rats. Brain structure & function. 2018;223(4):1829-38.

9 Hinova-Palova DV, Edelstein L, Landzhov B, Minkov M, Malinova L, Hristov S, et al. Topographical distribution and morphology of NADPH-diaphorase-stained neurons in the human claustrum. Frontiers in systems neuroscience. 2014;8:96.

10 Druga R, Smythies J, Edelstein L, Ramachandran V. The Claustrum: Structural, Functional, and Clinical Neuroscience. The Claustrum: Structural, Functional and Clinical Neuroscience, eds Smythies J R, Edelstein L R, Ramachandran V S 2014:29-84.

11 Wang Q, Ng L, Harris JA, Feng D, Li Y, Royall JJ, et al. Organization of the connections between claustrum and cortex in the mouse. The Journal of comparative neurology. 2017;525(6):1317-46.

12 Markowitsch HJ, Irle E, Bang-Olsen R, Flindt-Egebak P. Claustral efferents to the cat's limbic cortex studied with retrograde and anterograde tracing techniques. Neuroscience. 1984;12(2):409-25.

13 Brennan EKW, Jedrasiak-Cape I, Kailasa S, Rice SP, Sudhakar SK, Ahmed OJ. Thalamus and claustrum control parallel layer 1 circuits in retrosplenial cortex. eLife. 2021;10:e62207.

14 Stiefel KM, Merrifield A, Holcombe AO. The claustrum's proposed role in consciousness is supported by the effect and target localization of Salvia divinorum. Frontiers in integrative neuroscience. 2014;8:20.

15 Bayat A, Joshi S, Jahan S, Connell P, Tsuchiya K, Chau D, et al. A pilot study of the role of the claustrum in attention and seizures in rats. Epilepsy research. 2018;140:97-104.

16 Madden MB, Stewart BW, White MG, Krimmel SR, Qadir H, Barrett FS, et al. A role for the claustrum in cognitive control. Trends in cognitive sciences. 2022;26(12):1133-52.

17 Kurada L, Bayat A, Joshi S, Koubeissi MZ. The Claustrum in Relation to Seizures and Electrical Stimulation. Frontiers in neuroanatomy. 2019;13:8.

18 Wegiel J, Moryś J, Kowiański P, Ma SY, Kuchna I, Nowicki K, et al. Chapter 8 - Delayed Development of the Claustrum in Autism. In: Smythies JR, Edelstein LR, Ramachandran VS, editors. The Claustrum. San Diego: Academic Press; 2014. p. 225-35.

19 Kalaitzakis ME. Chapter 12 - Parkinson's Disease and the Claustrum. In: Smythies JR, Edelstein LR, Ramachandran VS, editors. The Claustrum. San Diego: Academic Press; 2014. p. 277-97.

20 Yanes JA, Riedel MC, Ray KL, Kirkland AE, Bird RT, Boeving ER, et al. Neuroimaging meta-analysis of cannabis use studies reveals convergent functional alterations in brain regions supporting cognitive control and reward processing. Journal of Psychopharmacology. 2018;32(3):283-95.

21 Acheson A, Ray KL, Hines CS, Li K, Dawes MA, Mathias CW, et al. Functional activation and effective connectivity differences in adolescent marijuana users performing a simulated gambling task. Journal of addiction. 2015;2015:783106.

22 Zarrindast MR, Khakpai F. The Modulatory Role of Dopamine in Anxiety-like Behavior. Archives of Iranian medicine. 2015;18(9):591-603.

23 Terem A, Gonzales BJ, Peretz-Rivlin N, Ashwal-Fluss R, Bleistein N, Del Mar Reus-Garcia M, et al. Claustral Neurons Projecting to Frontal Cortex Mediate Contextual Association of Reward. Current biology : CB. 2020;30(18):3522-32.e6.

24 Niu M, Kasai A, Tanuma M, Seiriki K, Igarashi H, Kuwaki T, et al. Claustrum mediates bidirectional and reversible control of stress-induced anxiety responses. Science advances. 2022;8(11):eabi6375.

25 Kim DH, Kim NJ, Zhao RJ, Kim DH, Yang CH, Kim HY, et al. Effects of acupuncture on the anxiety-like behavior induced by withdrawal from chronic morphine use. Neuroscience letters. 2018;664:38-42.

26 Chae Y, Yeom M, Han J-H, Park H-J, Hahm D-H, Shim I, et al. Effect of acupuncture on anxiety-like behavior during nicotine withdrawal and relevant mechanisms. Neuroscience letters. 2008;430(2):98-102.

27 Amorim D, Amado J, Brito I, Fiuza SM, Amorim N, Costeira C, et al. Acupuncture and electroacupuncture for anxiety disorders: A systematic review of the clinical research. Complementary therapies in clinical practice. 2018;31:31-37.

28 Zeng L, Tao Y, Hou W, Zong L, Yu L. Electro-acupuncture improves psychiatric symptoms, anxiety and depression in methamphetamine addicts during abstinence: A randomized controlled trial. Medicine. 2018;97(34):e11905.

29 Nie J, Wei X, Xu X, Li N, Li Y, Zhao Y, et al. Electro-acupuncture alleviates adolescent cocaine exposure-enhanced anxiety-like behaviors in adult mice by attenuating the activities of PV interneurons in PrL. FASEB journal : official publication of the Federation of American Societies for Experimental Biology. 2020;34(9):11913-24.

30 Shapo GR, Ma L, Liu C. [Effects of acupuncture at Weizhong (BL40) on brain function with PET/CT]. Zhongguo Zhong xi yi jie he za zhi Zhongguo Zhongxiyi jiehe zazhi = Chinese journal of integrated traditional and Western medicine. 2006;26(11):969-72.

31 Spear LP. The adolescent brain and age-related behavioral manifestations. Neuroscience and biobehavioral reviews. 2000;24(4):417-63.

32 Estelles J, Lluch J, Rodríguez-Arias M, Aguilar MA, Miñarro J. Cocaine exposure during adolescence affects anxiety in adult mice. Brain research bulletin. 2007;71(4):393-403.

33 Lopez B, Turner RJ, Saavedra LM. Anxiety and risk for substance dependence among late adolescents/young adults. Journal of anxiety disorders. 2005;19(3):275-94.

34 Jackson J, Karnani MM, Zemelman BV, Burdakov D, Lee AK. Inhibitory Control of Prefrontal Cortex by the Claustrum. Neuron. 2018;99(5):1029-39.e4.

35 Zingg B, Dong HW, Tao HW, Zhang LI. Input-output organization of the mouse claustrum. The Journal of comparative neurology. 2018;526(15):2428-43.

36 Siemsen BM, Lombroso PJ, McGinty JF. Intra-prelimbic cortical inhibition of striatal-enriched tyrosine phosphatase suppresses cocaine seeking in rats. Addiction biology. 2018;23(1):219-29.

37 Valzachi MC, Teodorov E, Marcourakis T, Bailey A, Camarini R. Enhancement of Behavioral Sensitization, Anxiety-Like Behavior, and Hippocampal and Frontal Cortical CREB Levels Following Cocaine Abstinence in Mice Exposed to Cocaine during Adolescence. PloS one. 2013;8(10):e78317.

38 Caffino L, Giannotti G, Messa G, Mottarlini F, Fumagalli F. Repeated cocaine exposure dysregulates BDNF expression and signaling in the mesocorticolimbic pathway of the adolescent rat. The world journal of biological psychiatry : the official journal of the World Federation of Societies of Biological Psychiatry. 2019;20(7):531-44.

39 Caffino L, Mottarlini F, Mingardi J, Zita G, Barbon A, Fumagalli F. Anhedonic-like behavior and BDNF dysregulation following a single injection of cocaine during adolescence. Neuropharmacology. 2020;175:108161.

40 Kim DH, Kim NJ, Zhao RJ, Kim DH, Yang CH, Kim HY, et al. Effects of acupuncture on the anxiety-like behavior induced by withdrawal from chronic morphine use. Neuroscience letters. 2018;664:38-42.

41 Shao F, Du J, Wang S, Cerne R, Fang J, Shao X, et al. Electroacupuncture Alleviates Anxiety-like Behavior in Pain Aversion Rats by Attenuating the Expression of Neuropeptide Y in Anterior Cingulate Cortex. Clinical Complementary Medicine and Pharmacology. 2022;2(2):100019.

42 Wu M, Chen Y, Shen Z, Zhu Y, Xiao S, Zhu X, et al. Electroacupuncture Alleviates Anxiety-Like Behaviors Induced by Chronic Neuropathic Pain via Regulating Different Dopamine Receptors of the Basolateral Amygdala. Molecular neurobiology. 2022.

Figure legends

Figure 1. ACE enhances anxiety with evoked claustrum and D1R^{CaMKII} in mice of adulthood. A, Experimental timeline. **B**, EPM test. **C**, OFT. **D**, MBT. **E**, Total protein levels of c-Fos. **F**, The percentage and number of c-Fos-positive & CaMKII-positive neurons. Scale bar, 300 μm/50 μm. **G,** The expression of D1R^{CaMKII}. Scale bar, 200 μm/50 μm. **H**, The mRNA levels of *D1R, D2R and D3R*. **I,** The protein levels of D1R, D2R and D3R. **J,** Levels of p-ERK$_{1/2}$ and ERK$_{1/2}$. **K,** Levels of p-CREB, CREB and BDNF. ASE, adolescent saline exposure; ACE, adolescent cocaine exposure; CL, claustrum. N.S., $p > 0.05$, *, $p < 0.05$, **, $p < 0.01$ vs ASE.

Figure 2. Blocking D1R within claustrum suppresses ACE-increased anxiety and claustrum activation in mice of adulthood. A, Experimental timeline and local injections of SCH-23390 into claustrum. Scale bar, 400/100 μm. **B**, EPM test. **C**, OFT. **D**, NSFT. **E,** The number of c-Fos-positive neurons. Scale bar, 100 μm. Vehicle, vehicle-treated ACE mice; SCH-23390, SCH-23390-treated ACE mice; CL, claustrum. N.S., $p > 0.05$, *, $p < 0.05$, **, $p < 0.01$ vs Vehicle.

Figure 3. Knocking-down D1R^{CaMKII} of claustrum suppresses ACE-increased anxiety and claustrum activation in mice of adulthood. A, Experimental design and timeline. **B**, Local injections of virus into claustrum. Scale bar, 300 μm. **C**, The D1R protein level. **D**, EPM test. **E**, OFT. **F**, NSFT. **G**, The percentage of c-Fos-positive neurons in EGFP-transfected neurons and the mean gray value of c-Fos in EGFP-transfected neurons. Scale bar, 400 μm/50 μm. ACE, adolescent cocaine exposure; ACE$_{Ctrl}$, ACE mice injected with

control virus; ACE_{KD}, ACE mice injected with knockdown virus; CL, claustrum. N.S., $p > 0.05$, *, $p < 0.05$, **, $p < 0.01$ vs ACE_{Ctrl}.

Figure 4. EA treatment rescues ACE-increased anxiety in mice of adulthood by suppressing claustrum activation and $D1R^{CaMKII}$. A, Experimental design and timeline. **B**, Schematic diagram of EA and SEA treatments in mice. **C**, EPM test. **D**, OFT. **E**, NSFT. **F**, The percentage and number of c-Fos-positive & CaMKII-positive neurons. Scale bar, 300 μm/50 μm. **G**, The D1R protein level. **H**, The staining of $D1R^{CaMKII}$. Scale bar, 200 μm/50 μm. **I**, Levels of p-$ERK_{1/2}$ and $ERK_{1/2}$. **J**, Levels of p-CREB, CREB and BDNF. ACE_{SEA}, sham electro-acupuncture-treated ACE mice; ACE_{EA}: electro-acupuncture (GV 20 and GV 29)-treated ACE mice; CL, claustrum. N.S., $p > 0.05$, *, $p < 0.05$, **, $p < 0.01$ vs ACE_{SEA}.

Figure 5. Schematic summary of present study. Adolescent cocaine exposure (ACE) enhances anxiety-like behaviors in mice of adult, accompanied with triggered activation of CaMKII-positive neurons and more dopamine receptor 1 (D1R) on CaMKII-positive neurons ($D1R^{CaMKII}$) in claustrum. Either blocking D1R with SCH23390 or knocking-down $D1R^{CaMKII}$ with virus in the claustrum efficiently reduce claustrum activation, and ultimately suppresses ACE-induced anxiety in mice. By targeting claustral $D1R^{CaMKII}$, electro-acupuncture (EA) at acupoints of GV20 and GV29 rescues ACE-increased anxiety in mice of adulthood. In the process, the p-CREB and BDNF may be the potential subsequent signals to $D1R^{CaMKII}$.